

# Identification of source locations for atmospheric dry deposition of heavy metals during yellow-sand events in Seoul, Korea in 1998 using hybrid receptor models

Young-Ji Han<sup>a</sup>, Thomas M. Holsen<sup>a</sup>, Philip K. Hopke<sup>b</sup>, Jang-Pyo Cheong<sup>c</sup>,  
Ho Kim<sup>d</sup>, Seung-Muk Yi<sup>d,\*</sup>

<sup>a</sup>*Department of Civil and Environmental Engineering, Clarkson University, Potsdam, NY 13699, USA*

<sup>b</sup>*Department of Chemical Engineering, Clarkson University, Potsdam, NY 13699, USA*

<sup>c</sup>*Department of Civil and Environmental Engineering, Kyung Sung University, Pusan, South Korea*

<sup>d</sup>*School of Public Health and the Institute of Health and Environment, Seoul National University, 28 Yeongon-dong, Chongro-gu, Seoul 110-799, South Korea*

Received 8 September 2003; received in revised form 23 January 2004; accepted 9 February 2004

---

## Abstract

Elemental dry deposition fluxes were measured using dry deposition plates from March to June 1998 in Seoul, Korea. During this spring sampling period several yellow-sand events characterized by long-range transport from China and Mongolia impacted the area. Understanding the impact of yellow-sand events on atmospheric dry deposition is critical to managing the heavy metal levels in the environment in Korea. In this study, the measured flux of a primarily crustal metal, Al and an anthropogenic metal, Pb was used with two hybrid receptor models, potential source contribution function (PSCF) and residence time weighted concentration (RTWC) for locating sources of heavy metals associated with atmospheric dry deposition fluxes during the yellow-sand events in Seoul, Korea.

The PSCF using a criterion value of the 75th percentile of the measured dry deposition fluxes and RTWC results using the measured elemental dry deposition fluxes agreed well and consistently showed that there were large potential source areas in the Gobi Desert in China and Mongolia and industrial areas near Tianjin, Tangshan, and Shenyang in China. Major industrial areas of Shenyang, Fushun, and Anshan, the Central China loess plateau, the Gobi Desert, and the Alashan semi-desert in China were identified to be major source areas for the measured Pb flux in Seoul, Korea. For Al, the main industrial areas of Tangshan, Tianjin and Beijing, the Gobi Desert, the Alashan semi-desert, and the Central China loess plateau were found to be the major source areas. These results indicate that both anthropogenic sources such as industrial areas and natural sources such as deserts contribute to the high dry deposition fluxes of both Pb and Al in Seoul, Korea during yellow-sand events.

RTWC resolved several high potential source areas. Modeling results indicated that the long-range transport of Al and Pb from China during yellow-sand events as well as non-yellow-sand spring daytimes increased atmospheric dry deposition of heavy metals in Korea.

© 2004 Elsevier Ltd. All rights reserved.

*Keywords:* Hybrid receptor models; Heavy metals; Dry deposition flux; Yellow-sand events; China; Korea; Seoul

---

\*Corresponding author. Tel.: +82-2-740-8879; Fax: +82-2-745-9105  
E-mail address: [yiseung@snu.ac.kr](mailto:yiseung@snu.ac.kr) (S.-M. Yi).

## 1. Introduction

Atmospheric deposition is defined as the process by which atmospheric pollutants are transferred to terrestrial and aquatic surfaces (Valigura et al., 1996) and is commonly classified as either dry or wet. The interest in atmospheric deposition has increased over the past decade due to concerns about the effects of deposited materials on the environment. Atmospheric dry deposition influences the fate of airborne toxics and often controls the transfer of material from the atmosphere to natural surfaces. Dry deposition provides a significant mechanism for the removal of particles from the atmosphere and is an important pathway for the loading of toxic trace metals and heavy metals into the aquatic ecosystem (Caffrey et al., 1998).

Pollutants emitted into the atmosphere can be transported and deposited to aquatic/terrestrial reservoirs far away from their original sources. For instance, soil particles from deserts and exposed regions can be blown up by strong winds behind cyclones and delivered to the free troposphere by the westerly jet and transported 5000–10,000 km eastwards over the North Pacific Ocean (Zhang et al., 1992). This material is called yellow-sand due to its yellowish, light brown, or red color and is mostly observed in the spring when large-scale dust storms occur in northern China and Mongolia (Duce and Unni, 1980; Nagoya University, 1991). The origin of yellow-sand is from large deserts including Taklamakan (330,000 km<sup>2</sup>), Gobi (60,000 km<sup>2</sup>), and Badain Jaran (44,300 km<sup>2</sup>) in China and Mongolia. Both Japan and Korea are affected by the long-range transport of dust from the west during yellow-sand events. The impact of these events can even be observed at elevated sites in the western United States (Liu et al., 2003).

Most research studies of yellow-sand events have attempted to identify the source regions and to simulate the transport of yellow-sand (Iwasaka et al., 1983; Kai et al., 1988; Yoon, 1990; Ishizaka, 1987; Tanaka et al., 1989; Lee et al., 1993; Kotamarthi and Carmichael, 1993; Chun et al., 2001). A recent study indicated that during yellow-sand events in 1998, typical soil constituents and anthropogenic elements were transported and deposited in Seoul, Korea (Yi et al., 2001). They found that among the elements analyzed the Pb flux had the most significant increase; its flux was approximately 4 times higher than during non-yellow-sand events.

To reduce the concentration of a certain pollutant, the main sources that impact the interested area must be identified. There have been numerous attempts to identify source types and source locations using receptor modeling. Hybrid receptor modeling combining back-trajectories originating from the receptor sites

and measured concentrations of interest is a powerful tool to locate source areas (Hopke, 1991; Ashbaugh et al., 1985; Keeler, 1987; Stohl, 1996; Seibert et al., 1994; Hopke, 2003). However, there have not been any previous efforts to locate possible source regions of the heavy metal dry deposition during yellow-sand events, partly because there are high uncertainties associated with dry deposition sampling techniques and the complexity of estimating dry deposition (Fisher and Oppenheimer, 1991; Pratt et al., 1996).

The main objective of this study is to identify possible source locations affecting the atmospheric dry deposition of heavy metals during yellow-sand events by combining air parcel back trajectories and direct measurements of dry deposition flux.

## 2. Models

### 2.1. Potential source contribution function (PSCF)

The PSCF receptor model was originally developed by Ashbaugh et al. (1985) and Malm et al. (1986). Both chemical and meteorological data for each sample are required for PSCF. In PSCF the area around the receptor site is dividing into a set of uniform sized grid cells. The PSCF model counts each trajectory segment endpoint that terminates within a given grid cell. The probability of an event at the receptor site is related to the number of endpoints in that cell relative to the total number of endpoints for all of the sample dates. If the number of endpoints that fall in the  $ij$ th cell is  $n(i, j)$  and the endpoints in the same grid cell when the concentrations are higher than a selected criterion value is  $m(i, j)$ , the PSCF value for the  $ij$ th cell is then defined as  $PSCF(i, j) = m(i, j)/n(i, j)$ . Grid cells that have high PSCF values are regarded as possible source locations. Cells containing emission sources would be identified with conditional probabilities close to one if trajectories that have crossed the cells effectively transport the emitted contaminant to the receptor site. The PSCF model thus provides a means to map the source potentials of geographical areas.

### 2.2. Residence time weighted concentration (RTWC)

In PSCF, a large source cannot be distinguished from a moderate source since only one criteria value is used. To avoid this problem, Seibert et al. (1994) developed a method imposing the weighted concentration onto each grid.

$$\overline{C_{mi}} = \frac{1}{\sum_{l=1}^M \tau_{mnl}} \sum_{l=1}^M \log(c_l) \tau_{mnl}, \quad (1)$$

where  $m, n$  are the indices of the horizontal grid,  $l$  is the index of the trajectory,  $M$  the total number of trajectories,  $c_l$  the concentration observed on arrival of trajectory  $l$  and  $\tau_{mnl}$  the time spent in grid elements  $(m, n)$  by trajectory  $l$ . Logarithmic concentrations were used because the concentrations followed an approximately lognormal distribution. In the RTWC model, a redistribution of concentration was proposed after computing a simple concentration field  $\overline{C_{mn}}$ , because the measured concentration is attributed equally to all segments in Eq. (1), whereas sources are often concentrated in hot spots (Stohl, 1996). Let  $c_l$  be the concentration measured upon arrival of trajectory  $l$  that is split into  $N_l$  segments with 1 h length. In addition,  $X_{il}$ ,  $i = 1, N_l$  is defined as the mean concentrations of the grid cells hit by segments of trajectory  $l$  and  $\overline{X_l}$  the average of the mean concentrations of the grid cells hit by segments  $j = 1, N_l$  of trajectory  $l$ :

$$\overline{X_l} = \frac{\sum_{j=1}^{N_l} X_{jl}}{N_l}. \quad (2)$$

The redistributed concentrations along trajectory  $l$  are

$$c_{il} = c_l \frac{X_{il} N_l}{\sum_{j=1}^{N_l} X_{jl}} = c_l \frac{X_{il}}{\overline{X_l}}, \quad i = 1, N_l. \quad (3)$$

After the redistribution is finished for all of the trajectories, the concentration field is computed as follows:

$$\overline{C_{mn}} = \frac{1}{\sum_{l=1}^M \sum_{i=1}^{N_l} \tau_{mnl}} \sum_{l=1}^M \sum_{i=1}^{N_l} \log(c_{il}) \tau_{mnl}, \quad (4)$$

where  $\tau_{mnl}$  is the residence time of segment  $i$  of trajectory  $l$  in grid cell  $(m, n)$ . With this new concentration field, a second redistribution of the concentrations along the trajectories is performed. This procedure is repeated until the average difference between the concentration fields of two successive iterations is below the desired value.

### 2.3. Application

The hybrid single-particle Lagrangian integrated trajectory model (Draxler and Hess, 1998; HYSPLIT4, 1997) was used in this study to obtain three-dimensional 3-day backward trajectories. An arrival height of 1000 m at the receptor location was used since yellow-sand events were assumed to be long-range transported. Areas that had only a few trajectory endpoints were removed with a point filter, in order to increase the confidence level of the result. In this study, cells having end points  $< 5$  were eliminated. Trajectories were calculated every 2 h for all samples.

## 3. Materials and methods

In this study, dry deposition was collected with a grease-coated smooth plate with a sharp leading edge similar to those used in previous studies (Holsen and Noll, 1992; Paode et al., 1998; Sofuoglu et al., 1998).

### 3.1. Sampling

Samples were collected on the roof of the Asan Engineering Building at Ewha Women's University, a five-story building located in a mixed institutional, commercial, and residential area in Seoul, Korea. Dry deposition fluxes and ambient particle size distributions were measured simultaneously during the daytime (from 09:00 to 18:00) and nighttime (from 18:00 to 09:00) during dry periods. (One of the daytime samples was collected over 2 days for a total of 18 h). Meteorological data were obtained every 5 min at the sampling site on a meteorological tower.

The particulate dry deposition flux was measured with Mylar strips (5.7 cm  $\times$  1.8 cm exposed surface area) coated with Apezion L grease ( $\sim 5 \mu\text{m}$  thick, 4 mg mass) attached to smooth acrylic plates. These plates had sharp leading edges ( $< 10^\circ$  angle) pointed into the wind by a wind vane. The sharp leading edge provided laminar flow over the strips thereby minimizing turbulent deposition. The greased surface eliminated particle bounce while collecting particles of all sizes. The strips were weighed before and after exposure to determine the total mass of particles collected (Paode et al., 1998; Sofuoglu et al., 1998). The dry deposition mass flux was calculated by dividing the measured difference in the greased strip mass before and after sampling by the greased area and sampling time.

Sample collection started on March 1998 and concluded in June 1998. Yellow-sand events occurred for a total of 13 days in 1998, 5 days and two nights of which were sampled.

### 3.2. Analysis

Analytical methods followed the procedures outlined by Paode et al. (1998) and Sofuoglu et al. (1998). Briefly, the grease and associated particles from the deposition strips were washed into Teflon containers and digested with an ultra-pure nitric acid solution in a microwave oven at 70 psi (CEM MDS-2000). Samples were subsequently analyzed for Al, Ca, Cu, Mn, Ni, Pb, and Zn with a Varian Ultramass 700 inductively coupled plasma—mass spectrometer (ICP-MS) in the Research Center of Natural Science located in Wonju, Korea.

### 3.3. Quality assurance/quality control

Method detection limits (MDLs) were calculated by injecting a low concentration sample seven times into the ICP-MS. MDLs were defined as three times the standard deviation of the concentrations obtained in the seven runs. MDLs for Pb and Al were 0.009 ppb ( $0.42 \mu\text{g m}^{-2}$ ) and 0.106 ppb ( $5.17 \mu\text{g m}^{-2}$ ), respectively. Metal concentrations in the process blanks were either below or of the same magnitude as the MDLs. Typical sample concentrations were 10 times MDLs.

Background contamination was routinely monitored using operational blanks (unexposed Mylar strips), which were processed simultaneously with field samples. At least 10% of the samples were analyzed in duplicate and spiked with a known amount of metal to calculate recovery efficiencies. No significant contamination was found (<5% of the levels found in the samples) and recovery efficiencies averaged 95% and varied between 83% and 107%.

## 4. Results and discussion

In this study, a  $1^\circ \times 1^\circ$  grid was used. The two models (PSCF and RTWC) were used to identify the source areas that impacted the dry deposition flux measured at the sampling site. There was generally no predominant

wind direction for the spring; however, northwesterly wind was slightly more common. Since the dry deposition flux was significantly elevated especially for Pb during yellow-sand events, hybrid receptor models were run for all flux samples measured during non yellow-sand spring daytimes as well as yellow-sand events to determine the source locations associated with the increased fluxes during yellow-sand events.

### 4.1. Dry deposition flux measurements

Over the study periods, the elemental dry deposition fluxes of Pb and Al ranged from 2.30 to  $322 \mu\text{g m}^{-2} \text{day}^{-1}$  and from 449 to  $8800 \text{mg m}^{-2} \text{day}^{-1}$ , respectively (Table 1). Six samples for each element were taken during yellow-sand events among the 20 samples. Considering only daytime fluxes, the average Pb flux during yellow-sand events ( $199 \mu\text{g m}^{-2} \text{day}^{-1}$ ) was about 4.7 times higher than during non-yellow-sand periods in the spring, while the average Al flux was approximately 1.5 times higher during the yellow-sand events ( $5400 \mu\text{g m}^{-2} \text{day}^{-1}$ ). Al is assumed to be a primarily crustal element; however, Pb is mostly from anthropogenic sources. Most of the aerosols transported from China during yellow-sand events are fine particles that can be transported a long distance. Al particles transported from China during yellow-sand events were mostly in particles <  $10 \mu\text{m}$  in size and these particles do

Table 1  
Summary of atmospheric dry deposition flux data used in this study

	Day/night	Sampling date	Sampling duration (min)	Dry deposition flux ( $\mu\text{g m}^{-2} \text{day}^{-1}$ )	
				Al	Pb
Yellow-sand event	Day	4/14/1998	522	3810	161
	Day	4/16/1998	485	8800	322
	2 Day	4/19–20/1998	985	3220	31.6
	Day	4/21/1998	499	5760	280
	Night	4/20/1998	946	1340	4.53
	Night	4/21/1998	930	549	76.1
				3910	146
<i>Average</i>					
Non-yellow-sand	2 Days	3/16–17/1998	1191	6970	44.6
Spring daytime	2 Days	3/31, 23/1998	1051	2910	15.1
	2 Days	4/2–3/1998	985	4700	53.1
	Day	4/29/1998	425	1210	25.8
	Day	5/4/1998	500	449	2.30
	Day	5/6/1998	540	1710	88.8
	Day	5/9/1998	520	2490	3.56
	Day	5/18/1998	545	2410	50.8
	Day	5/27/1998	565	1450	87.2
	Day	5/29/1998	573	7190	33.4
	Day	5/30/1998	585	6520	129
	Day	6/8/1998	532	4310	34.8
	Day	6/9/1998	545	3440	2.37
	Day	6/11/1998	582	3690	15.1
	<i>Average</i>				3530

not contribute significantly to dry deposition flux that is primarily controlled by particles  $> 10 \mu\text{m}$  (Holsen et al., 1993; Paode et al., 1998; Sofuoglu et al., 1998). On the other hand, the increase in the concentrations of Pb mostly associated with particles  $< 10 \mu\text{m}$  in size during yellow-sand events resulted in high dry deposition fluxes.

Measured Al fluxes were on average 1–2 orders of magnitude higher than the fluxes of Pb, and this finding is in good agreement with previous studies (Yi et al., 2001; Paode et al., 1998). During the nighttime, significantly lower fluxes were observed for both elements possibly due to the low ambient concentration and low wind velocity. The lower concentrations may have resulted from a shallow nighttime inversion layer that prevented mixing of dust-loaded upper air down to the surface.

From the back trajectory analysis, the trajectories for the nighttime during yellow-sand events do not correspond to the high PSCF and RTWC values indicating that dry deposition fluxes during the night were not related to the possible source regions that are linked to high dry deposition fluxes.

## 4.2. PSCF

### 4.2.1. Source locations of Pb

In this study, the criterion value was set to the 75th percentile of dry deposition flux measurements in order to identify high emission sources. PSCF results using all of the flux measurements during yellow-sand events and non yellow-sand spring daytime measurements are shown in Fig. 1. Since the Pb flux was much higher during yellow-sand events, the samples greater than the

criterion value were mostly taken during yellow-sand events. Sources contributing to the high Pb flux at the sampling site during spring time of 1998 were identified to be the Gobi Desert, the Alashan semi-desert, the Central China loess plateau, and major industrial areas in China. The Gobi Desert is the second largest desert in China and assumed to be the main source of yellow-sand transported to Korea.

The PSCF results represent potential source directions rather than locations because PSCF modeling evenly distributes weight along the path of trajectories (Hsu et al., 2003). Therefore, the so-called trailing effect generally appears, especially when PSCF is performed for a single sampling site or with a limited sample number so that areas upwind and downwind of actual sources are also likely to be indicated to be possible source areas. In most cases, the trailing effect is recognized to be a drawback of PSCF modeling. However, it can be useful in locating the pathway between the source areas and the receptor site. Four pathways from the sources to the sampling site were resolved by PSCF when high dry deposition fluxes of Pb were measured (Fig. 1). Directions from the Gobi Desert, the Central China loess plateau, the Pacific Ocean, and the major industrial areas that produce high Pb emissions including Shenyang, Fushun, Anshan, Dalian, and Liaoyang in China were clearly shown. This result strongly indicates that the high Pb fluxes measured during yellow-sand events were attributed not only to the deserts in China but also to the industrial areas, particularly when the northwesterly wind was observed. During yellow-sand events, Pb particles produced in industrial areas were likely mixed in with

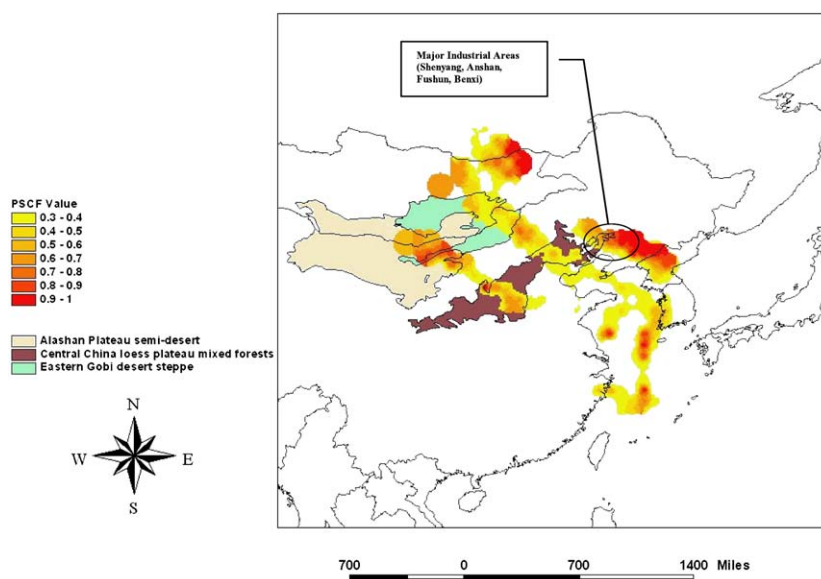


Fig. 1. Likely source areas impacting the Pb dry deposition flux in Seoul, Korea over the study period using PSCF modeling.

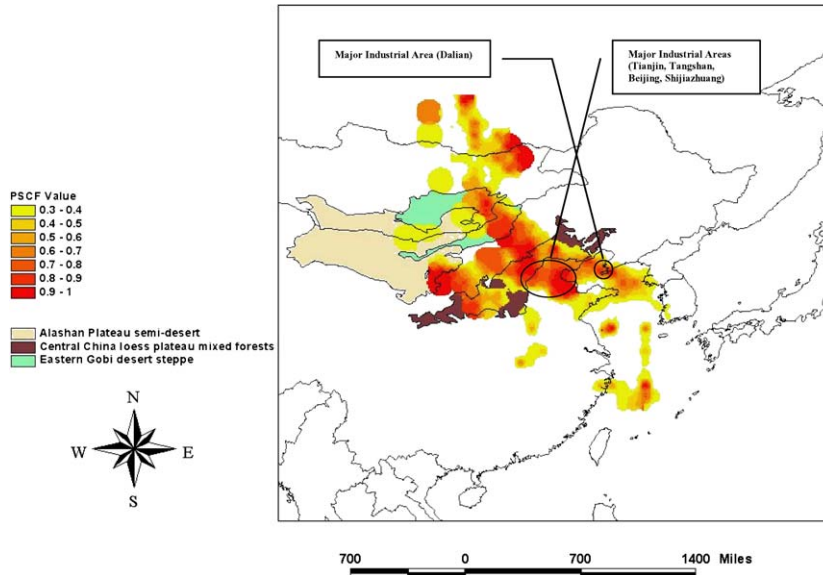


Fig. 2. Likely source areas impacting the Al dry deposition flux in Seoul, Korea over the study period using PSCF modeling.

the extremely high concentration of fine particles that originated from deserts during yellow-sand events. These large quantities of lead particles were transported to the receptor site in Seoul, Korea, resulting in the wide source areas around the industrial areas shown in Fig. 1.

#### 4.2.2. Source locations of Al

The 75th percentile of the measured Al flux included one sample from yellow-sand events and four samples from non yellow-sand spring daytime. Therefore, the PSCF results for Al flux will indicate the likely source locations impacting high Al dry deposition flux during yellow-sand events as well as non yellow-sand spring daytimes.

PSCF resolved the Gobi Desert, the Central China loess plateau, and major industrial areas including Tianjin, Tangshan, Beijing, and Shijiazhuang in China as the main Al sources that impacted the dry deposition flux of Al in Seoul, Korea (Fig. 2). Compared with the PSCF results for Pb, the possible source areas for Al flux were more widely distributed. Wider source locations for Al around the desert areas were attributed to the fact that Al is primarily a crustal element. This wider pathway from sources to the receptor site appeared since only one Al sample during yellow-sand events was bigger than the criterion value, so that the source areas during non yellow-sand events were also identified. Sources affecting the Al dry deposition flux in Seoul, Korea were not easily distinguishable between yellow-sand events and non yellow-sand spring daytimes.

Major source locations of the measured Al flux were very similar to those for the measured Pb flux including the Gobi Desert and the Central China loess plateau.

However, the locations of anthropogenic sources for each element were different, as mentioned earlier, and PSCF modeling was able to precisely identify those locations for each element.

#### 4.3. Residence time weighted concentration (RTWC)

##### 4.3.1. Source locations of Pb

The main differences between RTWC modeling and PSCF are that the logarithmic concentration (or flux) is directly related to the trajectories and the concentration (or flux) is redistributed not only over the number of trajectories, but also over the number of segments of each trajectory. This feature of RTWC makes the identification of “hot spots” possible. In this study, a point filter for the minimum number of samples crossing a grid cell was not used since only a limited number of samples were available.

The flux gradients generated by RTWC do not represent the actual contributions from these areas, but show the relative importance of source locations (Hsu et al., 2003). Major source locations identified by RTWC for Pb (Fig. 3) were very similar to the PSCF results, including the Central China loess plateau, the Alashan semi-desert, and major industrial areas. The direct pathway from the Gobi Desert to the receptor site shown in PSCF results (Fig. 1) did not appear in the RTWC result, indicating that the Gobi Desert may only be a moderate source. Sources in the industrial areas near Shenyang, Fushun, Anshan, Dalian, and Liaoyang were also identified to be high potential source regions in RTWC.

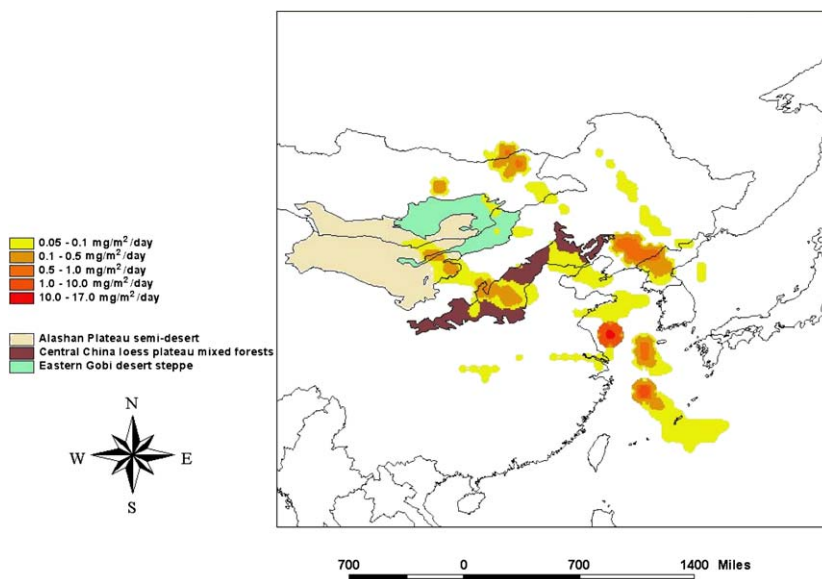


Fig. 3. Likely source areas impacting the Pb dry deposition flux in Seoul, Korea over the study period using RTWC modeling.

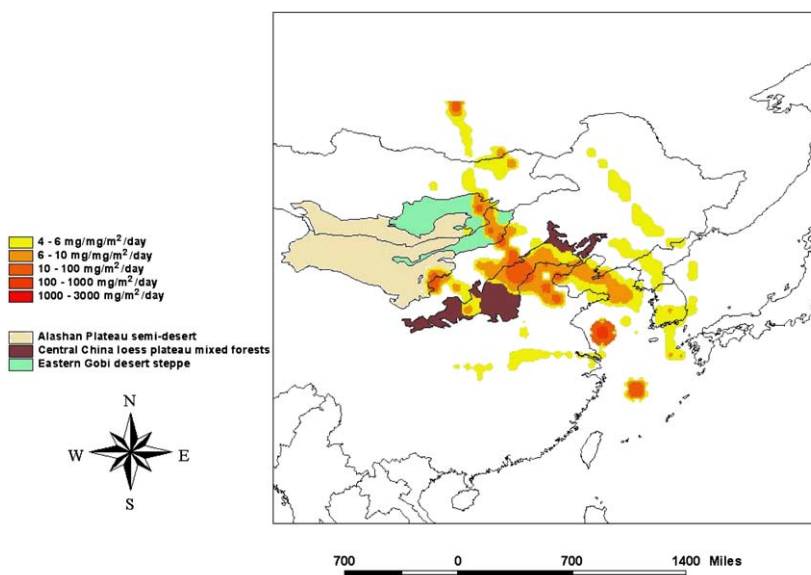


Fig. 4. Likely source areas impacting the Al dry deposition flux in Seoul, Korea over the study period using RTWC modeling.

#### 4.3.2. Source locations of Al

The flux regenerated by RTWC increased by about 3 orders of magnitude over the original flux value, producing strong spatial gradients in the field compared to PSCF. The RTWC results for Al dry deposition flux were similar to the PSCF result (Fig. 4) and indicated there were potential sources in the Gobi Desert, the Alashan semi-desert, the Central China loess plateau, and industrial areas in China. The RTWC result, however, showed an improved separation be-

tween large and small source areas. The major industrial areas including Tianjin, Tangshan, Beijing, and Shijiazhuang were identified to be the source area in PSCF as well, but in RTWC, three hot spots in this industrial region were specifically resolved. Also, the areas located between the Gobi Desert and the Central China loess plateau were suggested to be large source areas in PSCF modeling because of the trailing effect. These areas were mostly eliminated in the RTWC results (Fig. 4).

Compared with the measured Pb dry deposition flux results, the central China loess plateau was suggested to be a more important source for Al. This result indicates that the Al flux was more strongly associated with sources closer to the receptor site possibly because Al is associated with larger particles than is Pb.

Both PSCF and RTWC showed sources areas over the ocean for Al and Pb fluxes. From the back trajectory analysis, two trajectories out of five trajectories on 16 April 1998 showed very slow air movement over the ocean west of Seoul. This slow air movement resulted in a large number of endpoints and high PSCF values for this region. In addition, many trajectories associated with high dry deposition fluxes (high PSCF and RTWC values) from yellow-sand events passed over this area resulting in being identified as a possible source region (sometimes called a “trailing effect” as indicated above). Since the PSCF and RTWC models are based on statistical analysis, this modeling artifact can be eliminated if the number of samples is large enough. Therefore, if the number of samples is not large enough, the model results should be analyzed carefully considering other analysis techniques such as the back trajectory analysis.

## 5. Conclusions

The elemental dry deposition fluxes of Pb and Al were directly measured using a grease-coated smooth plate with a sharp leading edge in Seoul, Korea during the spring in 1998. Yellow-sand events that seriously deteriorated the air quality in Korea were observed during this sampling period and the measured fluxes during yellow-sand events significantly increased.

To identify the source locations associated with the high fluxes of Pb and Al, two trajectory-based models, PSCF and RTWC, were used. Both PSCF and RTWC resolved similar source locations for both elements; however, RTWC indicated smaller source regions without trailing effects while PSCF showed the source direction rather than the precise source location. Major industrial areas of Shenyang, Fushun, and Anshan, the Central China loess plateau, the Gobi Desert, and the Alashan semi-desert in China were identified to be major source areas for the measured Pb flux in Seoul, Korea. For Al, the main industrial areas of Tangshan, Tianjin and Beijing, the Gobi Desert, the Alashan semi-desert, and the Central China loess plateau were found to be the major source areas. Sources affecting the Al dry deposition flux in Seoul, Korea were not easily distinguishable between yellow-sand events and non yellow-sand spring daytimes. These results indicate that anthropogenic sources such as industrial areas as well as natural sources such as deserts contribute to the high dry deposition fluxes of both Pb and Al in Seoul, Korea

during yellow-sand events as well as non yellow-sand spring daytimes.

## Acknowledgements

This work was funded in part by the Ministry of Environment, Republic of Korea (Ecotechnopia 2002-02310-0002-0).

## References

- Ashbaugh, L.L., Malm, W.C., Sadeh, W.D., 1985. A residence time probability analysis of sulfur concentrations at Grand Canyon National Park. *Atmospheric Environment* 19, 1263–1270.
- Caffrey, P.F., Ondov, J.M., Zufall, M.J., Davidson, C.I., 1998. Determination of size-dependent dry deposition velocities with multiple intrinsic elemental tracers. *Environmental Science and Technology* 32, 1615–1622.
- Chun, Y.S., Boo, K.O., Kim, J.Y., Park, S.U., Lee, M.H., 2001. Synopsis, transport, and physical characteristics of Asian dust in Korea. *Journal of Geophysical Research* 106 (D16–18), 461–469.
- Draxler, R.R., Hess, G.D., 1998. An overview of the HYSPLIT\_4 modelling system for trajectories, dispersion, and deposition. *Australian Meteorological Magazine* 47, 295–308.
- Duce, R.A., Unni, C.K., 1980. Long-range atmospheric transport of soil dust from Asia to the Tropical North Pacific: temporal variability. *Science* 209, 1522–1524.
- Fisher, D.C., Oppenheimer, M., 1991. Atmospheric nitrogen deposition and the Chesapeake Bay Estuary. *AMBIO: A Journal of the Human Environment* 20 (3), 102–108.
- Holsen, T.M., Noll, K.E., 1992. Dry deposition of atmospheric particles, application of current models to ambient data. *Environmental Science and Technology* 26, 1807–1815.
- Holsen, T.M., Noll, K.E., Fang, G.C., Lee, W.J., Lin, J.M., 1993. Dry deposition and particle size distributions measured during the Lake Michigan Urban air toxics study. *Environmental Science and Technology* 27, 1327–1333.
- Hopke, P.K., 1991. Receptor modeling for air quality management. Elsevier, Amsterdam.
- Hopke, P.K., 2003. Recent developments in receptor modeling. *Journal of Chemometrics* 17, 255–265.
- Hsu, Y.K., Holsen, T.M., Hopke, P.K., 2003. Comparison of hybrid receptor models to locate PCB sources in Chicago. *Atmospheric Environment* 37, 545–562.
- HYSPLIT4 (Hybrid Single-Particle Lagrangian Integrated Trajectory) Model, 1997. NOAA Air Resources Laboratory, Silver Spring, MD, <http://www.arl.noaa.gov/ready/hysplit4.html>.
- Ishizaka, Y., 1987. Chemical–physical process of Kosa particles’ surface during long-range transport. *Tenki* 34, 179–182 (in Japanese).
- Iwasaka, Y., Minoura, H., Nagaya, K., 1983. The transport and spatial scale of Asian dust-storm clouds: a case study of the dust-storm event of April 1979. *Tellus* 35B, 189–196.

- Kai, K., Okada, Y., Uchino, O., Tabata, I., Nakamura, H., Takasugi, T., Nikaidou, Y., 1988. Lidar observation and numerical simulation of A Kosa (Asian Dust) over Tsukuba, Japan during the spring of 1986. *Journal of Meteorological Society of Japan* 66, 457–472.
- Keeler, G.J., 1987. A hybrid approach for source apportionment of atmospheric pollutants in the Northeastern United State, Ph.D. Thesis, University of Michigan.
- Kotamarthi, V.R., Carmichael, G.R., 1993. A modeling study of the long-range transport of Kosa using particle trajectory methods. *Tellus* 45B, 426–441.
- Lee, J.G., Kim, Y.H., Kim, J.S., 1993. A case study of the yellow-sand phenomenon observed over the Korean Peninsula for 1–3 April 1993. *Journal of Atmospheric Research* 10 (1), 51–73 (in Korean).
- Liu, W., Hopke, P.K., VanCuren, R.A., 2003. Origins of fine aerosol mass in the western united states using positive matrix factorization. *Journal of Geophysical Research-Atmosphere* 108 (D23), 4716–4733.
- Malm, W.C., Johnson, C.E., Bresch, J.F., 1986. Application of principal component analysis for purposes of identifying source–receptor relationships in receptor methods for source apportionment. In: Pace, T.G. (Ed.), *Air Pollution Control Association*. Pittsburgh, PA, pp. 127–148.
- Nagoya University, 1991. Kosa, 328pp (in Japanese).
- Paode, R.D., Sofuoglu, S.C., Sivadechathep, J., Noll, K.E., Holsen, T.M., 1998. Dry deposition fluxes and mass size distributions of Pb, Cu, and Zn measured in Southern Lake Michigan during AEOLOS. *Environmental Science and Technology* 32, 1629–1635.
- Pratt, G.C., Orr, E.J., Bock, D.C., Strassman, R.L., Fundine, D.W., Twaroski, C.J., Thornton, J.D., Meyers, T.P., 1996. Estimation of dry deposition of inorganics using filter pack data and inferred deposition velocity. *Environmental Science & Technology* 30, 2168–2177.
- Seibert, P., Kromp-Kolb, H., Baltensperger, U., Jost, D.T., Schwikowski, M., Kasper, A., Puxbaum, H., 1994. Trajectory analysis of aerosol measurements at high alpine sites. In: Borrell, P.M., Borell, P., Cvitas, T., Seiler, W. (Eds.), *Transport and Transformation of Pollutants in the Troposphere*. Academic Publishing, Den Haag, pp. 689–693.
- Sofuoglu, S.C., Paode, R.D., Sivadechathep, J., Noll, K.E., Holsen, T.M., Keeler, G.J., 1998. Dry deposition fluxes and atmospheric size distributions of mass, Al and Mg measured in Southern Lake Michigan during AEOLOS. *Journal of Aerosol Science and Technology* 29 (4), 281–293.
- Stohl, A., 1996. Trajectory statistics—A new method to establish source–receptor relationships of air pollutants and its application to the transport of particulate sulfate in Europe. *Atmospheric Environment* 30, 579–587.
- Tanaka, M., Shiobara, M., Nakajama, T., Yamano, M., 1989. Aerosol optical characteristics in the Yellow Sand Events observed in May, 1982 at Nagasaki-Part I observations. *Journal of Meteorological Society of Japan* 19, 267–278.
- Valigura, R.A., Winston, T.L., Artz, R.S., Hicks, B.B., 1996. *Atmospheric Nutrient Input To Coastal Areas-Reducing the Uncertainties*. NOAA Coastal Ocean Program Decision Analysis Series No. 9. NOAA Coastal Ocean Office, Silver Spring, MD. 24pp. + 4 appendices.
- Yi, S.M., Eun-Young, Lee, Holsen, T.M., 2001. Dry deposition fluxes and size distribution of heavy metals in Seoul, Korea During yellow-sand events. *Aerosol Science and Technology* 35 (1), 569–576.
- Yoon, Y.H., 1990. On the yellow-sand transported to the Korean Peninsula. *Journal of Meteorological Society of Korea* 26, 111–120 (in Korean).
- Zhang, J., Huang, W.W., Liu, S.M., Liu, M.G., Yu, Q., Wang, J.H., 1992. Transport of particulate heavy metals towards the China Sea: a preliminary study and comparison. *Marine Chemistry* 40 (3), 161–178.